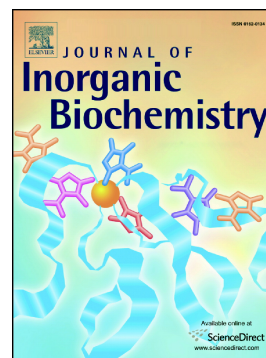


## Accepted Manuscript

Synthesis and biological evaluation of substituted 3-(2'-benzimidazolyl)coumarin platinum(II) complexes as new telomerase inhibitors

Ting Meng, Qi-Pin Qin, Zhen-Rui Wang, Li-Ting Peng, Hua-Hong Zou, Zhen-Yuan Gan, Ming-Xiong Tan, Kai Wang, Fu-Pei Liang



PII: S0162-0134(18)30245-9  
DOI: doi:[10.1016/j.jinorgbio.2018.09.004](https://doi.org/10.1016/j.jinorgbio.2018.09.004)  
Reference: JIB 10559

To appear in: *Journal of Inorganic Biochemistry*

Received date: 27 April 2018  
Revised date: 8 September 2018  
Accepted date: 9 September 2018

Please cite this article as: Ting Meng, Qi-Pin Qin, Zhen-Rui Wang, Li-Ting Peng, Hua-Hong Zou, Zhen-Yuan Gan, Ming-Xiong Tan, Kai Wang, Fu-Pei Liang , Synthesis and biological evaluation of substituted 3-(2'-benzimidazolyl)coumarin platinum(II) complexes as new telomerase inhibitors. Jib (2018), doi:[10.1016/j.jinorgbio.2018.09.004](https://doi.org/10.1016/j.jinorgbio.2018.09.004)

This is a PDF file of an unedited manuscript that has been accepted for publication. As a service to our customers we are providing this early version of the manuscript. The manuscript will undergo copyediting, typesetting, and review of the resulting proof before it is published in its final form. Please note that during the production process errors may be discovered which could affect the content, and all legal disclaimers that apply to the journal pertain.

**Synthesis and biological evaluation of substituted  
3-(2'-benzimidazolyl)coumarin platinum(II) complexes as new  
telomerase inhibitors**

Ting Meng <sup>a</sup>, Qi-Pin Qin <sup>a,b,\*</sup>, Zhen-Rui Wang <sup>a</sup>, Li-Ting Peng <sup>a</sup>, Hua-Hong Zou <sup>a,\*</sup>,  
Zhen-Yuan Gan <sup>a</sup>, Ming-Xiong Tan <sup>b,\*</sup>, Kai Wang <sup>c</sup>, Fu-Pei Liang <sup>a,c,\*</sup>

<sup>a</sup> *State Key Laboratory for the Chemistry and Molecular Engineering of Medicinal Resources, School of Chemistry and Pharmacy, Guangxi Normal University, 15 Yucui Road, Guilin 541004, PR China. E-mail: gxnuchem@foxmail.com (H.-H. Zou); fliangoffice@yahoo.com (F.-P. Liang).*

<sup>b</sup> *Guangxi Key Lab of Agricultural Resources Chemistry and Biotechnology, College of Chemistry and Food Science, Yulin Normal University, 1303 Jiaoyudong Road, Yulin 537000, PR China. qpqin2018@126.com (Q.-P. Qin); mxtan2018@126.com (M.-X. Tan).*

<sup>c</sup> *Guangxi Key Laboratory of Electrochemical and Magnetochemical Functional Materials, College of Chemistry and Bioengineering, Guilin University of Technology, Guilin 541004, China.*

**Abstract**

Eight new platinum(II) complexes **Pt1–Pt8** with substituted 3-(2'-benzimidazolyl) coumarins were successfully synthesized and characterized by single crystal X-ray diffraction analysis, nuclear magnetic resonance spectroscopy (NMR), electrospray ionization-mass spectrometry (ESI-MS), infrared spectrophotometry (IR) and elemental analysis. Crystallographic data of these **Pt1–Pt8** complexes showed that the Pt(II) has distorted four-coordinated square planar geometry. **Pt1–Pt8** were found to display high cytotoxic activity *in vitro* against the cisplatin-resistant SK-OV-3/DDP cancer cells with a low IC<sub>50</sub> from 1.01–10.32  $\mu$ M, but low cytotoxicity on the normal HL-7702 cells. Further studies revealed that **Pt1–Pt3** induced apoptosis in SK-OV-3/DDP cancer cells *via* mitochondria dysfunction signaling pathways. Our findings also indicated that **Pt1** was a telomerase inhibitor targeting c-myc promoter elements.

**Keywords:** 3-(2'-benzimidazolyl)coumarins, platinum(II) complexes, cell apoptosis, telomerase activity, mitochondrial dysfunction

## 1. Introduction

In the last few decades, Pt-based drugs such as cisplatin, carboplatin and oxaliplatin have been developed for the treatment of various cancers [1, 2]. However, Pt-based anticancer drugs exhibit drug resistance and severe side effects in the therapeutic process. This fact has motivated researchers to search for more effective, less toxic, and target-specific platinum-based anticancer drugs [3–6]. For example, Lippard investigated *trans*-[Pt(NH<sub>3</sub>)<sub>2</sub>(phenanthridine)Cl]NO<sub>3</sub> displays significant antitumor properties, with a different spectrum of activity than that of classic bifunctional cross-linking agents like cisplatin [7–11]. Hambley and co-authors reported that *trans*-[Pt(OH)<sub>2</sub>(ox)(en)] (ox= OAc, en= 1,2-ethylenediamine) more cytotoxic against human A2780 tumor cells (human ovarian cancer cell line) than against DLD-1 cancer cells (human colon cancer cell line) [12–16]. Farrell suggested that [Pt(dien)L]<sup>2+</sup> (dien= N'-[2-(dimethylamino)ethyl]-N,N-dimethylethylenediamine, L= nucleobase or nucleoside) gave especially strong  $\pi$ - $\pi$  stacking interactions with tryptophan and the tryptophan-containing C-terminal zinc finger (ZF) of the HIV nucleocapsid protein NCp7 [17–20]. Collins and Wheate demonstrated that cisplatin@CB[7] and *trans*-[PtCl(NH<sub>3</sub>)<sub>2</sub>]<sub>2</sub>(m-NH<sub>2</sub>(CH<sub>2</sub>)<sub>8</sub>NH<sub>2</sub>)<sup>2+</sup> (CT008) is just as effective on A2780 tumor cells and a delivery mechanism for controlled slow release of large dinuclear ruthenium(II) complexes, respectively [21–23].

Previous reports have shown that telomerase is overexpressed in 85–90% of the human tumor cells but has undetectable activity in most of the human normal somatic cells [24, 25]. Thus, the design of Pt-based drugs to interfere with or target telomerase activity in cancer cells is a promising approach to discover potential anticancer agents [26]. For example, Mao et al. reported that flexible trinuclear Pt(II) complexes are effective and selective G4 binders and good telomerase inhibitors [27]. Yan and

co-authors reported the high binding selectivity and affinity ( $\sim 10^7 \text{ dm}^3 \cdot \text{mol}^{-1}$ ) of this dipyridophenazine (dppz) Pt(II) complex toward the G-quadruplex, as well as its nanomolar potency against telomerase ( $^{Tel}IC_{50} = 760 \text{ nM}$ ). Vilar et al. investigated mono-substituted phenanthroline platinum(II) square planar complexes and showed that they induce a high degree of quadruplex DNA stabilization and inhibit telomerase activity [28].

Coumarin and its derivatives are important naturally occurring products and they have wide-range applications as agrochemicals and drugs such as anticancer, antituberculosis, anti-HIV, anti-inflammatory, anti-Alzheimer's, anti-influenza, antiviral and antimicrobial agents [29,30]. Nevertheless, the metal complexes of coumarin and its derivatives are rarely explored as telomerase inhibitors [31–34]. On the basis of the previous studies, in order to exploit new Pt(II) complexes with different coordination mode and more extended planar coumarin ligand, by means of combining the potential of Pt(II) complexes as anticancer agents and the significant bioactivity of alkaloids, herein, we firstly reported that the Pt(II) complexes [Pt(MeOBC)(DMSO)Cl<sub>2</sub>] (**Pt1**), [Pt(OHBC)(DMSO)Cl<sub>2</sub>] (**Pt2**), [Pt(BC)(DMSO)Cl<sub>2</sub>] (**Pt3**), [Pt(FBC)(DMSO)Cl<sub>2</sub>] (**Pt4**), [Pt(BrBC)(DMSO)Cl<sub>2</sub>] (**Pt5**), [Pt(FFBC)(DMSO)Cl<sub>2</sub>] (**Pt6**), [Pt(ClClBC)(DMSO)Cl<sub>2</sub>] (**Pt7**) and [Pt(BrBrBC)(DMSO)Cl<sub>2</sub>] (**Pt8**) with eight ligands 3-(2'-benzimidazolyl)-8-methoxycoumarin (MeOBC), 3-(2'-benzimidazolyl)-8-hydroxycoumarin (OHBC), 3-(2'-benzimidazolyl)coumarin (BC), 3-(2'-benzimidazolyl)-7-fluorocoumarin (FBC), 3-(2'-benzimidazolyl)-7-bromocoumarin (BrBC), 3-(2'-benzimidazolyl)-6,8-difluorocoumarin (FFBC), 3-(2'-benzimidazolyl)-6,8-dichlorocoumarin (ClClBC) and 3-(2'-benzimidazolyl)-6,8-dibromocoumarin (BrBrBC) were synthesized and fully characterized. By

assessing their cytotoxicity against HeLa (human sarcoma HeLa cancer cell line), Hep-G2 (human hepatocellular carcinoma cell line), SK-OV-3/DDP (human cisplatin-resistant SK-OV-3 cell line), SK-OV-3 (human ovarian cancer cell line) tumor cells and human normal HL-7702 cells (human normal hepatocytes cell line), we proposed a possible antitumor mechanism.

## 2. Results and Discussion

### 2.1 Synthesis and Characterization

As shown in Scheme 1, the eight ligands MeOBC, OHBC, BC, FBC, BrBC, FFBC, ClCIBC and BrBrBC were synthesized according to the reported procedures [35,36]. After synthesizing these ligands, the Pt(II) complexes [Pt(MeOBC)(DMSO)Cl<sub>2</sub>] (**Pt1**), [Pt(OHBC)(DMSO)Cl<sub>2</sub>] (**Pt2**), [Pt(BC)(DMSO)Cl<sub>2</sub>] (**Pt3**), [Pt(FBC)(DMSO)Cl<sub>2</sub>] (**Pt4**), [Pt(BrBC)(DMSO)Cl<sub>2</sub>] (**Pt5**), [Pt(FFBC)(DMSO)Cl<sub>2</sub>] (**Pt6**), [Pt(ClCIBC)(DMSO)Cl<sub>2</sub>] (**Pt7**) and [Pt(BrBrBC)(DMSO)Cl<sub>2</sub>] (**Pt8**) were synthesized by the direct reaction of MeOBC, OHBC, BC, FBC, BrBC, FFBC, ClCIBC and BrBrBC with *cis*-Pt(DMSO)<sub>2</sub>Cl<sub>2</sub>, respectively, in a mixture of CH<sub>3</sub>OH and DMSO at 90 °C for 48 h. These ligands and their Pt(II) complexes were characterized by single crystal X-ray diffraction analysis, <sup>1</sup>H NMR, ultraviolet-visible (UV-Vis), ESI-MS, IR and elemental analysis (Fig. S1–S48). Furthermore, **Pt1–Pt8** were demonstrated to be stable for 48 h in TBS (10 mM Tris-HCl buffer containing 1% DMSO, pH = 7.35) by UV-Vis spectroscopy (Fig. S41).

#### [Scheme 1]

### 2.2 Crystal structures of Pt1–Pt8

As shown in Figs. 1 and S42–S48, the Pt(II) centers of Pt(II) complexes **Pt1–Pt8** adopt four coordinated square planar geometry and are surrounded by one substituted

3-(2'-benzimidazolyl)coumarin (MeOBC, OHBC, BC, FBC, BrBC, FFBC, ClCIBC or BrBrBC), two chloride and one DMSO. The selected crystallographic information of the Pt(II) complexes **Pt1–Pt8** are summarized in Tables S1–S20. The Pt–N, Pt–S and Pt–Cl distances are in the ranges of 2.0370 to 2.0640 Å, 2.2111 to 2.2239 Å and 2.2856 to 2.3102 Å, respectively (Tables S1–S20), which are within the normal range.

[Fig. 1]

### 2.3 *In vitro* cell cytotoxicity

The *in vitro* cytotoxicity of *cis*-Pt(DMSO)<sub>2</sub>Cl<sub>2</sub>, cisplatin, the ligands MeOBC, OHBC, BC, FBC, BrBC, FFBC, ClCIBC and BrBrBC, as well as the Pt(II) complexes **Pt1–Pt8**, against a panel of human HeLa, Hep-G2, SK-OV-3/DDP, SK-OV-3 tumor cell lines and normal HL-7702 cells were evaluated by 3-(4,5-dimethylthiazol-2-yl)-2,5-diphenyltetrazolium bromide (MTT) assay (Tables 1 and S21). Against the selected cancer cell lines, the inhibitory rates of **Pt1–Pt8** were higher than that of MeOBC, OHBC, BC, FBC, BrBC, FFBC, ClCIBC, BrBrBC and *cis*-Pt(DMSO)<sub>2</sub>Cl<sub>2</sub>, respectively (Table S21). As reported in Table 1, **Pt1** showed the highest cytotoxicity against all the selected cancer cell lines and the cytotoxicity of metal complexes followed the order of **Pt1>Pt2>Pt4>Pt5>Pt6>Pt7>Pt8>Pt3**. Such observed different antiproliferative effects can be due to the influence of the electronic effect of the methoxy, hydroxyl and halogen substituted group of MeOBC, OHBC, BC, FBC, BrBC, FFBC, ClCIBC and BrBrBC in the Pt(II) complexes **Pt1–Pt8** [37]. Importantly, **Pt1–Pt8** showed overall higher *in vitro* cytotoxicity than that of cisplatin towards human SK-OV-3/DDP tumor cells, with IC<sub>50</sub> values from 1.01–10.32 μM. The SK-OV-3/DDP cell line was the most sensitive to **Pt1–Pt8**. Furthermore, the Pt(II) complexes **Pt1–Pt8** displayed low cytotoxicity towards normal HL-7702 cells, which suggested their potential cytotoxic selectivity for SK-OV-3/DDP tumor cells. In

addition, **Pt1** (1.0  $\mu\text{M}$ ), about 43.0% of the SK-OV-3/DDP tumor cells underwent cell apoptotic phase, whereas in the case of cisplatin (70.0  $\mu\text{M}$ ), **Pt2** (3.0  $\mu\text{M}$ ) and **Pt3** (10.0  $\mu\text{M}$ ) treated cells, only 8.2%, 19.1% and 11.2% underwent apoptosis, respectively (Figs. 8 and S50). Therefore, **Pt1** (1.0  $\mu\text{M}$ ), **Pt2** (3.0  $\mu\text{M}$ ) and **Pt3** (10.0  $\mu\text{M}$ ) were selected for the in vitro antitumor mechanism assays in SK-OV-3/DDP tumor cells for 24 h.

#### [Table 1]

### 2.4 TRAP-silver staining assay

It has been reported that inhibition of telomerase activity by Pt-based drugs may lead to continuous telomere shortening followed by growth arrest and cell apoptosis in the cancer cells [39,40]. Here, we compared the ability of **Pt1** (1.0  $\mu\text{M}$ ), **Pt2** (3.0  $\mu\text{M}$ ), **Pt3** (10.0  $\mu\text{M}$ ), **Pt4** (3.0  $\mu\text{M}$ ) and **Pt5** (10.0  $\mu\text{M}$ ) to inhibit the telomerase activity in the SK-OV-3/DDP cancer cells by the telomeric repeat amplification protocol (TRAP)-silver staining assay. As shown in Fig. 2, the Pt(II) complex **Pt1** (1.0  $\mu\text{M}$ ) was shown to be highly active in the inhibition of the telomerase activity with an inhibitory rate of 52.28%, and that by **Pt2** (3.0  $\mu\text{M}$ ), **Pt3** (10.0  $\mu\text{M}$ ), **Pt4** (3.0  $\mu\text{M}$ ) and **Pt5** (10.0  $\mu\text{M}$ ) were 39.57%, 35.90%, 14.55% and 11.82%, respectively.

#### [Fig. 2]

### 2.5 Cellular uptake

Previous studies have suggested that the biological activity of Pt-based drugs was strongly dependent on the accumulation in tumor cells [41–48]. Because of the weak inhibitory activity of **Pt4** (3.0  $\mu\text{M}$ ) and **Pt5** (10.0  $\mu\text{M}$ ) in telomerase activity assay, only **Pt1** (1.0  $\mu\text{M}$ ), **Pt2** (3.0  $\mu\text{M}$ ) and **Pt3** (10.0  $\mu\text{M}$ ) were studied. The cellular uptake assay for **Pt1** (1.0  $\mu\text{M}$ ), **Pt2** (3.0  $\mu\text{M}$ ), **Pt3** (10.0  $\mu\text{M}$ ) and cisplatin (15.0  $\mu\text{M}$ ) were conducted in SK-OV-3/DDP tumor cells, and the accumulation of platinum (Pt) was

examined by inductively coupled plasma mass spectrometry (ICP-MS) assay, which were performed as Sadler and Lippard *et al* reported [41–48]. Notably, the uptake of **Pt1** ( $6.52 \pm 0.26$  nmol of Pt/ $10^6$  cells) appeared to increase steadily over the course of 24 h, and its concentration was higher than that of Pt detected in the SK-OV-3/DDP cells treated with **Pt2** ( $(5.18 \pm 0.12$  nmol of Pt)/ $10^6$  cells), **Pt3** ( $(4.35 \pm 0.05$  nmol of Pt)/ $10^6$  cells) and cisplatin ( $(4.11 \pm 0.18$  nmol of Pt)/ $10^6$  cells) under the same condition (Fig. 3).

[Fig. 3]

## 2.6 Effects of Pt1–Pt3 on c-myc and hTERT transcription and expression

Western blot, Reverse Transcription Polymerase Chain Reaction (RT-PCR) assay and transfection were performed [49–52] to investigate whether the Pt(II) complexes **Pt1** ( $1.0 \mu\text{M}$ ), **Pt2** ( $3.0 \mu\text{M}$ ) and **Pt3** ( $10.0 \mu\text{M}$ ) could affect the transcription and expression of the oncoprotein c-myc and human telomerase reverse transcriptase gene (hTERT), consequently inhibiting the telomerase activity. Firstly, we explored the effects of Pt(II) complexes **Pt1** ( $1.0 \mu\text{M}$ ), **Pt2** ( $3.0 \mu\text{M}$ ), **Pt3** ( $10.0 \mu\text{M}$ ) on the mRNA and protein levels of c-myc and hTERT. As shown in Figs. 4A-C, Western blot and RT-PCR analysis revealed that **Pt1** ( $1.0 \mu\text{M}$ ), **Pt2** ( $3.0 \mu\text{M}$ ) and **Pt3** ( $10.0 \mu\text{M}$ ), especially **Pt1** ( $1.0 \mu\text{M}$ ), reduced the mRNA and protein levels of c-myc and hTERT in the SK-OV-3/DDP tumor cells. Furthermore, after successful transfection of enhanced green fluorescent protein (EGFP) and c-myc plasmid vector, **Pt1** ( $1.0 \mu\text{M}$ ) exhibited a remarkable decrease in the emission of the bright green fluorescence of a luciferase reporter (Figs. 4D and E). The inhibition of the c-myc promoter in the SK-OV-3/DDP cells was in the following order: **Pt1**>**Pt2**>**Pt3**.

[Fig. 4]

## 2.7 Pt1–Pt3 increase levels of mitochondrial $\text{Ca}^{2+}$ fluctuation and triggers ROS

**generation**

Studies suggested that increased levels of mitochondrial  $\text{Ca}^{2+}$  stimulate mitochondrial reactive oxygen species (ROS) formation, which causes the opening of mPTP (mitochondrial permeability transition pore) and the complete collapse of mitochondria membrane potential (MMP) [53–55]. To determine whether **Pt1** (1.0  $\mu\text{M}$ ), **Pt2** (3.0  $\mu\text{M}$ ) and **Pt3** (10.0  $\mu\text{M}$ ) induce increase of mitochondrial  $\text{Ca}^{2+}$  and trigger ROS generation in SK-OV-3/DDP tumor cells, FACS analysis of mitochondrial  $\text{Ca}^{2+}$  fluctuation and ROS generation were carried out. As shown in Figs. 5A and B, treatments of SK-OV-3/DDP tumor cells with **Pt1** (1.0  $\mu\text{M}$ ), **Pt2** (3.0  $\mu\text{M}$ ) and **Pt3** (10.0  $\mu\text{M}$ ) for 24 h resulted in a pronounced increase of ROS level and  $\text{Ca}^{2+}$  fluctuation in the following order: **Pt1**>**Pt2**>**Pt3**. The results suggested that treatments with **Pt1** (1.0  $\mu\text{M}$ ), **Pt2** (3.0  $\mu\text{M}$ ) and **Pt3** (10.0  $\mu\text{M}$ ) led to an increase in ROS production, which may represent a critical step in the **Pt1** (1.0  $\mu\text{M}$ ), **Pt2** (3.0  $\mu\text{M}$ ) and **Pt3** (10.0  $\mu\text{M}$ ) induced apoptosis in human SK-OV-3/DDP tumor cells [53–55].

[Fig. 5]

**2.8 Pt1–Pt3 trigger apoptosis via the mitochondrial pathway**

To investigate the effects of **Pt1** (1.0  $\mu\text{M}$ ), **Pt2** (3.0  $\mu\text{M}$ ) and **Pt3** (10.0  $\mu\text{M}$ ) on mitochondrial function, we first measured MMP using the 5,5',6,6'-tetrachloro-1,1',3,3'-tetraethylbenzimidazolylcarbocyanine (JC-1) staining [53–55]. JC-1 is a fluorescent dye that accumulates selectively in mitochondria depending on the membrane potential. As shown in Fig. 6, exposure of SK-OV-3/DDP tumor cells to **Pt1** (1.0  $\mu\text{M}$ ), **Pt2** (3.0  $\mu\text{M}$ ) and **Pt3** (10.0  $\mu\text{M}$ ) for 24 h could cause disruption of MMP. In addition, flow cytometry and Western blot analysis showed that treating cells with **Pt1** (1.0  $\mu\text{M}$ ), **Pt2** (3.0  $\mu\text{M}$ ) and **Pt3** (10.0  $\mu\text{M}$ ) resulted in accumulated cytochrome c, decrease of bcl-2 level and increases of capase-3, bax,

apaf-1 and caspase-9 levels (Figs. 7 and S49). All these results demonstrated that **Pt1** (1.0  $\mu\text{M}$ ), **Pt2** (3.0  $\mu\text{M}$ ) and **Pt3** (10.0  $\mu\text{M}$ ) could induce a mitochondrion-mediated apoptotic pathway in SK-OV-3/DDP tumor cells [53–55].

[Fig. 6]

[Fig. 7]

## 2.9 Induction of apoptosis by Pt1–Pt3 in SK-OV-3/DDP cells

We determined whether **Pt1–Pt3**-mediated loss of SK-OV-3/DDP tumor cell viability was due to the induction of cell apoptosis [56, 57]. After exposure to **Pt1** (1.0  $\mu\text{M}$ ), about 43.0% of the SK-OV-3/DDP tumor cells underwent cell apoptotic phase, whereas in the case of **Pt2** (3.0  $\mu\text{M}$ ) and **Pt3** (10.0  $\mu\text{M}$ ) treated cells, 19.1% and 11.2% underwent apoptosis, respectively (Fig. 8). However, cisplatin (70.0  $\mu\text{M}$ ) did not significantly induce SK-OV-3/DDP tumor cell apoptosis (Q2+Q3, 8.17%) under the same conditions (Fig. S50). Therefore, **Pt1** (1.0  $\mu\text{M}$ ), **Pt2** (3.0  $\mu\text{M}$ ) and **Pt3** (10.0  $\mu\text{M}$ ) were selected for the in vitro antitumor mechanism assays in SK-OV-3/DDP tumor cells for 24 h.

[Fig. 8]

## Structure-Activity Relationships

Based on the above described results, the cytotoxic mechanism studies of different substituted 3-(2'-benzimidazolyl) coumarins ligands (MeOBC, OHBC, BC, FBC, BrBC, FFBC, ClClBC and BrBrBC) and eight new platinum(II) complexes **Pt1–Pt8**, certain SAR (structure-activity relationships) trends emerged among the different groups substituted in substituted 3-(2'-benzimidazolyl) coumarins ligands. Such observed different in vitro antitumor activity and antitumor mechanism can be due to the influence of the electronic effect of the methoxy, hydroxyl and halogen substituted group of MeOBC, OHBC, BC, FBC, BrBC, FFBC, ClClBC and BrBrBC

in the Pt(II) complexes **Pt1–Pt8** [37].

i) The in vitro antitumor activity was follow the order of MeOBC>OHBC>FBC>BrBC>FFBC>ClCIBC>BrBrBC>BC (or **Pt1>Pt2>Pt4>Pt5>Pt6>Pt7>Pt8>Pt3**).

ii) The telomerase activity was follow the order of MeOBC>OHBC>FBC>BrBC>BC (or **Pt1>Pt2>Pt4>Pt5>Pt3**).

iii) RT-PCR and Western blot of c-myc and hTERT, transfection and cell apoptosis, **Pt1–Pt3** increase levels of mitochondrial Ca<sup>2+</sup> fluctuation and triggers ROS generation, **Pt1–Pt3** caused mitochondrial dysfunction in SK-OV-3/DDP tumor cells as well as cellular uptake ability follow the order of MeOBC>OHBC>BC (or **Pt1>Pt2>Pt3**).

### 3. Conclusions

Eight new Pt(II) complexes [Pt(MeOBC)(DMSO)Cl<sub>2</sub>] (**Pt1**), [Pt(OHBC)(DMSO)Cl<sub>2</sub>] (**Pt2**), [Pt(BC)(DMSO)Cl<sub>2</sub>] (**Pt3**), [Pt(FBC)(DMSO)Cl<sub>2</sub>] (**Pt4**), [Pt(BrBC)(DMSO)Cl<sub>2</sub>] (**Pt5**), [Pt(FFBC)(DMSO)Cl<sub>2</sub>] (**Pt6**), [Pt(ClCIBC)(DMSO)Cl<sub>2</sub>] (**Pt7**) and [Pt(BrBrBC)(DMSO)Cl<sub>2</sub>] (**Pt8**) have been synthesized and fully characterized. **Pt1** exhibited selective cytotoxicity to SK-OV-3/DDP tumor cells, and it showed higher cytotoxicity than that of **Pt2–Pt8** and the corresponding substituted 3-(2'-benzimidazolyl)coumarins. Additionally, the Pt(II) complexes **Pt1–Pt3** increased the levels of ROS and mitochondrial Ca<sup>2+</sup> fluctuation, and induced the decrease of MMP, consequently causing mitochondrial dysfunction. Various experiments showed that **Pt1** was a telomerase inhibitor targeting c-myc promoter elements.

## 4. Experimental

### 4.1 Synthesis

#### 4.1.1 Synthesis of ligands

##### *Synthesis of MeOBC, OHBC and BC ligands*

The ligands MeOBC, OHBC and BC were synthesized according to the reported procedures [35,36].

##### *Synthesis of FBC, BrBC, FFBC, ClClBC and BrBrBC ligands*

2-cyanomethylbenzimidazole (0.01 mol) and 0.01 mol 4-fluoro-2-hydroxybenzaldehyde, 4-bromo-2-hydroxybenzaldehyde, 3,5-difluorosalicylaldehyde, 3,5-dichlorosalicylaldehyde or 3,5-dibromosalicylaldehyde were added to ethanol (30 mL). Piperidine (0.1 mL) was then added and the mixture stirred at 55 °C for 24 h. The yellow precipitate which gradually separated out of the solution was collected and heated under reflux in 2.0% aqueous hydrochloric acid solution (150 mL) for 6.0 h. The mixture was cooled and excess sodium acetate added. The resulting brown product of 3-(2'-benzimidazolyl)-7-fluorocoumarin (FBC), 3-(2'-benzimidazolyl)-7-bromocoumarin (BrBC), 3-(2'-benzimidazolyl)-6,8-difluorocoumarin (FFBC), 3-(2'-benzimidazolyl)-6,8-dichlorocoumarin (ClClBC) and 3-(2'-benzimidazolyl)-6,8-dibromocoumarin (BrBrBC) were suitable for structural characterization.

Characterization of FBC. Yield: 82.56%. ESI-MS  $m/z$ : 281.0  $[M+H]^+$ . Elemental analysis calcd (%) for  $C_{16}H_9FN_2O_2$ : C 68.57, H 3.24, N 10.00; found: C 68.65, H 3.31, N 9.89.  $^1H$  NMR (400 MHz,  $DMSO-d_6$ )  $\delta$  9.18 (s, 1H), 8.09 (dd,  $J = 8.7, 6.4$  Hz, 1H), 7.69 (dd,  $J = 6.1, 3.2$  Hz, 2H), 7.55 (dd,  $J = 9.6, 2.5$  Hz, 1H), 7.37 (td,  $J = 8.7, 2.5$  Hz, 1H), 7.27 (dd,  $J = 6.1, 3.2$  Hz, 2H).  $^{13}C$  NMR (101 MHz,  $DMSO-d_6$ )  $\delta$  166.25, 163.74, 159.33, 155.10, 154.96, 145.91, 142.78, 132.33, 132.22, 123.33, 116.58, 116.55,

115.99, 115.55, 113.85, 113.62, 104.58, 104.32, 40.63, 40.42, 40.21, 40.00, 39.79, 39.58, 39.38, 25.09.

Characterization of BrBC. Yield: 79.52%. ESI-MS  $m/z$ : 339.2  $[M-H]^-$ . Elemental analysis calcd (%) for  $C_{16}H_9BrN_2O_2$ : C 56.33, H 2.66, N 8.21; found: C 56.25, H 2.60, N 8.13.  $^1H$  NMR (400 MHz, DMSO- $d_6$ )  $\delta$  9.29 (s, 1H), 7.95 (d,  $J = 1.8$  Hz, 1H), 7.92 (d,  $J = 8.4$  Hz, 1H), 7.81 (dd,  $J = 6.1, 3.2$  Hz, 2H), 7.72 (dd,  $J = 8.3, 1.8$  Hz, 1H), 7.44 (dd,  $J = 6.1, 3.2$  Hz, 2H).  $^{13}C$  NMR (101 MHz, DMSO- $d_6$ )  $\delta$  158.40, 154.27, 144.83, 144.55, 131.73, 129.15, 127.77, 125.17, 120.03, 118.24, 115.51, 40.63, 40.42, 40.21, 40.00, 39.79, 39.58, 39.37.

Characterization of FFBC. Yield: 81.42%. ESI-MS  $m/z$ : 299.0  $[M+H]^+$ . Elemental analysis calcd (%) for  $C_{16}H_8F_2N_2O_2$ : C 64.43, H 2.70, N 9.39; found: C 64.52, H 2.77, N 9.25.  $^1H$  NMR (400 MHz, DMSO- $d_6$ )  $\delta$  12.59 (s, 1H), 9.13 (d,  $J = 1.2$  Hz, 1H), 7.85 – 7.73 (m, 2H), 7.69 (dd,  $J = 5.8, 3.4$  Hz, 2H), 7.28 – 7.22 (m, 2H).  $^{13}C$  NMR (101 MHz, DMSO- $d_6$ )  $\delta$  158.32, 145.55, 141.05, 121.61, 121.58, 121.49, 121.47, 119.28, 113.45, 110.90, 110.86, 110.65, 110.62, 108.60, 108.39, 108.31, 108.10, 40.62, 40.41, 40.20, 39.99, 39.78, 39.58, 39.37.

Characterization of ClClBC. Yield: 75.01%. ESI-MS  $m/z$ : 330.9  $[M+H]^+$ . Elemental analysis calcd (%) for  $C_{16}H_8Cl_2N_2O_2$ : C 58.03, H 2.43, N 8.46; found: C 58.10, H 2.39, N 8.39.  $^1H$  NMR (400 MHz, DMSO- $d_6$ )  $\delta$  9.14 (s, 1H), 8.13 (d,  $J = 2.4$  Hz, 1H), 8.05 (d,  $J = 2.4$  Hz, 1H), 7.72 (dd,  $J = 6.1, 3.2$  Hz, 2H), 7.29 (dd,  $J = 6.1, 3.2$  Hz, 2H).  $^{13}C$  NMR (101 MHz, DMSO- $d_6$ )  $\delta$  158.40, 148.20, 145.26, 141.36, 132.32, 129.21, 128.04, 123.63, 121.95, 121.32, 40.62, 40.42, 40.21, 40.00, 39.79, 39.58, 39.37, -15.55.

Characterization of BrBrBC. Yield: 79.63%. ESI-MS  $m/z$ : 418.9  $[M-H]^-$ . Elemental analysis calcd (%) for  $C_{16}H_8Br_2N_2O_2$ : C 45.75, H 1.92, N 6.67; found: C 45.70, H

2.00, N 6.64.  $^1\text{H}$  NMR (400 MHz,  $\text{DMSO-}d_6$ )  $\delta$  9.14, 8.27, 8.26, 8.25, 8.25, 8.24, 8.23, 8.03, 8.03, 8.02, 8.02, 7.77, 7.76, 7.73, 7.72, 7.72, 7.71, 7.70, 7.32, 7.31, 7.30, 7.29, 7.28, 7.28, 7.26, 7.21, 7.21, 2.52, 2.51, 2.51, 2.50, 2.50.  $^{13}\text{C}$  NMR (101 MHz,  $\text{DMSO-}d_6$ )  $\delta$  158.45, 149.69, 145.13, 141.55, 137.72, 131.55, 123.77, 122.28, 117.24, 110.64, 40.62, 40.42, 40.21, 40.00, 39.79, 39.58, 39.37.

#### 4.1.2 Synthesis of Pt1–Pt8

The Pt(II) complexes  $[\text{Pt}(\text{MeOBC})(\text{DMSO})\text{Cl}_2]$  (**Pt1**),  $[\text{Pt}(\text{OHBC})(\text{DMSO})\text{Cl}_2]$  (**Pt2**),  $[\text{Pt}(\text{BC})(\text{DMSO})\text{Cl}_2]$  (**Pt3**),  $[\text{Pt}(\text{FBC})(\text{DMSO})\text{Cl}_2]$  (**Pt4**),  $[\text{Pt}(\text{BrBC})(\text{DMSO})\text{Cl}_2]$  (**Pt5**),  $[\text{Pt}(\text{FFBC})(\text{DMSO})\text{Cl}_2]$  (**Pt6**),  $[\text{Pt}(\text{ClClBC})(\text{DMSO})\text{Cl}_2]$  (**Pt7**) and  $[\text{Pt}(\text{BrBrBC})(\text{DMSO})\text{Cl}_2]$  (**Pt8**) were prepared by treating MeOBC, OHBC, BC, FBC, BrBC, FFBC, ClClBC or BrBrBC (0.10 mmol) with *cis*-Pt(DMSO) $_2$ Cl $_2$  (0.10 mmol) in methanol (2.0 mL) and DMSO (0.5 mL) at 90 °C for 48 h, respectively. The yellow block crystals suitable for X-ray diffraction analysis were harvested.

Characterization of **Pt1**. Yield: 91.53%. ESI-MS  $m/z$ : 635.1  $[\text{M-H}]^-$ . Elemental analysis calcd (%) for  $\text{C}_{19}\text{H}_{18}\text{Cl}_2\text{N}_2\text{O}_4\text{PtS}$ : C 35.86, H 2.85, N 4.40; found: C 35.80, H 2.94, N 4.43. IR (KBr): 3311, 3024, 2924, 1713, 1604, 1577, 1467, 1436, 1272, 1121, 1104, 1032, 953, 778, 754, 537, 438  $\text{cm}^{-1}$ .

Characterization of **Pt2**. Yield: 80.69%. ESI-MS  $m/z$ : 621.0  $[\text{M-H}]^-$ . Elemental analysis calcd (%) for  $\text{C}_{18}\text{H}_{16}\text{Cl}_2\text{N}_2\text{O}_4\text{PtS}$ : C 34.74, H 2.59, N 4.50; found: C 34.65, H 2.67, N 4.43. IR (KBr): 3325, 3005, 1702, 1606, 1577, 1515, 1435, 1290, 1142, 1092, 1018, 976, 750, 730, 543, 510, 438  $\text{cm}^{-1}$ .

Characterization of **Pt3**. Yield: 76.22%. ESI-MS  $m/z$ : 605.1  $[\text{M-H}]^-$ . Elemental analysis calcd (%) for  $\text{C}_{18}\text{H}_{16}\text{Cl}_2\text{N}_2\text{O}_3\text{PtS}$ : C 35.65, H 2.66, N 4.62; found: C 35.60, H 2.73, N 4.59. IR (KBr): 3328, 3302, 3005, 1712, 1605, 1572, 1434, 1319, 1140, 1106, 1024, 741, 440  $\text{cm}^{-1}$ .

Characterization of **Pt4**. Yield: 70.88%. ESI-MS  $m/z$ : 623.0  $[M-H]^-$ . Elemental analysis calcd (%) for  $C_{18}H_{15}Cl_2FN_2O_3PtS$ : C 34.63, H 2.42, N 4.49; found: C 34.59, H 2.49, N 4.40. IR (KBr): 3319, 3235, 3006, 1706, 1609, 1575, 1509, 1420, 1235, 1132, 1023, 775, 732, 618, 492, 437  $cm^{-1}$ .

Characterization of **Pt5**. Yield: 95.03%. ESI-MS  $m/z$ : 685.0  $[M-H]^-$ . Elemental analysis calcd (%) for  $C_{18}H_{15}BrCl_2N_2O_3PtS$ : C 31.55, H 2.21, N 4.09; found: C 31.50, H 2.32, N 4.13. IR (KBr): 3393, 3288, 3021, 2925, 1720, 1594, 1400, 1314, 1133, 1062, 968, 727, 589, 438  $cm^{-1}$ .

Characterization of **Pt6**. Yield: 78.03%. ESI-MS  $m/z$ : 641.0  $[M-H]^-$ . Elemental analysis calcd (%) for  $C_{18}H_{14}Cl_2F_2N_2O_3PtS$ : C 33.66, H 2.20, N 4.36; found: C 33.60, H 2.29, N 4.30. IR (KBr): 3242, 3039, 1727, 1590, 1431, 1378, 1309, 1241, 1139, 1095, 969, 737, 677, 442  $cm^{-1}$ .

Characterization of **Pt7**. Yield: 83.56%. ESI-MS  $m/z$ : 675.0  $[M-H]^-$ . Elemental analysis calcd (%) for  $C_{18}H_{14}Cl_4N_2O_3PtS$ : C 32.02, H 2.09, N 4.15; found: C 31.89, H 2.00, N 4.26. IR (KBr): 3225, 1729, 1564, 1407, 1152, 1111, 1024, 992, 764, 737, 548, 434  $cm^{-1}$ .

Characterization of **Pt8**. Yield: 70.12%. ESI-MS  $m/z$ : 762.9  $[M-H]^-$ . Elemental analysis calcd (%) for  $C_{18}H_{14}Br_2Cl_2N_2O_3PtS$ : C 28.29, H 1.85, N 3.67; found: C 28.20, H 2.07, N 3.71. IR (KBr): 3206, 1727, 1614, 1555, 1448, 1401, 1247, 1150, 1110, 1023, 975, 935, 740, 528, 432  $cm^{-1}$ .

## 4.2 Materials and methods

The X-Ray crystallography structures of **Pt1–Pt8** were solved by Sheldrick method [58]. The in vitro antitumor mechanism assays of **Pt1–Pt8** were according to the reported procedures [59–64]. In addition, all the materials, instrumentation and the detailed procedures for other experimental methods were described in supporting

information.

### Abbreviations

TBS	Tris-HCl buffer
MTT	3-(4,5-dimethylthiazol-2-yl)-2,5-diphenyltetrazolium bromide
ROS	reactive oxygen species
IC <sub>50</sub>	half maximal inhibitory concentration
mPTP	mitochondrial permeability transition pore
MMP	mitochondria membrane potential
SK-OV-3/DDP	human cisplatin-resistant SK-OV-3 cells
cells	
Hep-G2 cells	human hepatocellular carcinoma cells
SK-OV-3 cells	human ovarian cancer cells
HeLa cells	human sarcoma HeLa cancer cells
HL-7702 cells	human normal hepatocytes cells
PI	propidium iodide
$\Delta\psi$	mitochondrial membrane potential
JC-1	5,5',6,6'-tetrachloro-1,1',3,3'-tetraethylbenzimidazolylcarbocyanine
ox	OAc
en	1,2-ethylenediamine
dien	N'-[2-(dimethylamino)ethyl]-N,N-dimethylethylenediamine

## Acknowledgement

This work was supported by the National Natural Science Foundation of China (Nos. 51572050, 21867017, 21601038, 21261025 and 21761033), the Natural Science Foundation of Guangxi (Nos. 2018GXNSFBA138021, 2015GXNSFDA139007 and 2016GXNSFAA380085), Guangxi Key Laboratory of Electrochemical and Magnetochemical Functional Materials (EMFM20162107), the Key Foundation Project of Colleges and Universities in Guangxi (No. ZD2014108), the PhD Research Startup Program of Yulin Normal University (No. G2017009) and the Innovative Team & Outstanding Talent Program of Colleges and Universities in Guangxi (2014-49).

## References

- [1] F.-U. Rahman, A. Ali, I.U. Khan, H.-Q. Duong, S.-B. Yu, Y.-J. Lin, H. Wang, Z.-T. Li, D.-W. Zhang, *Eur. J. Med. Chem.* 131 (2017) 263–274.
- [2] B. Rosenberg, L. Vancamp, J.E. Trosko, V.H. Mansour, *Nature* 222 (1969) 385–386.
- [3] Y.-S. Li, B. Peng, L. Ma, S.-L. Cao, L.-L. Bai, C.-R. Yang, C.-Q. Wan, H.-J. Yan, P.-P. Ding, Z.-F. Li, J. Liao, Y.-Y. Meng, H.-L. Wang, J. Li, X. Xu, *Eur. J. Med. Chem.* 127 (2017) 137–146.
- [4] A. Alama, B. Tasso, F. Novelli, F. Sparatore, *Drug Discov. Today* 14 (2009) 500–508.
- [5] M.K. Amir, S.Z. Khan, F. Hayat, A. Hassan, I.S. Butler, Zia-ur-Rehman, *Inorg. Chim. Acta* 451 (2016) 31–40.
- [6] X. Yan, T.R. Cook, P. Wang, F. Huang, P.J. Stang, *Nat. Chem.* 7 (2015) 342–348.
- [7] W. Zhou, M. Almeqdadi, M.E. Xifaras, I.A. Riddell, Ö.H. Yilmaz, S.J. Lippard, *Chem. Commun.* 54 (2018) 2788–2791.

- [8] P.M. Bruno, Y. Liu, G.Y. Park, J. Murai, C.E. Koch, T.J. Eisen, J.R. Pritchard, Y. Pommier, S.J. Lippard, M.T. Hemann, *Nat. Med.* 23 (2017) 461–471.
- [9] Y.-R. Zheng, K. Suntharalingam, T.C. Johnstone, S.J. Lippard, *Chem. Sci.* 6 (2016) 1189–1193.
- [10] T.C. Johnstone, K. Suntharalingam, S.J. Lippard, *Chem. Rev.* 116 (2016) 3436–3486.
- [11] D. Wang, S.J. Lippard, *Nat. Rev. Drug Discov.* 4 (2005) 307–320.
- [12] C.K.J. Chen, J.Z. Zhang, J.B. Aitken, T.W. Hambley, *J. Med. Chem.* 56 (2013) 8757–8764.
- [13] M.E. Graziotto, M.C. Akerfeldt, A.P. Gunn, K. Yang, M.V. Somerville, N.V. Coleman, B.R. Roberts, T.W. Hambley, E.J. New, *J. Inorg. Biochem.* 177 (2017) 328–334.
- [14] M.D. Hall, T.W. Hambley, *Coordinati. Chem. Rev.* 232 (2002) 49–67.
- [15] J.Z. Zhang, P. Bonnitca, E. Wexselblatt, A.V. Klein, Y. Najajreh, D. Gibson, T.W. Hambley, *Chem. Eur. J.* 19 (2013) 1672–1676.
- [16] M.D. Hall, H.L. Daly, J.Z. Zhang, M. Zhang, R.A. Alderden, D. Pursche, G.J. Foran, T.W. Hambley, *Metallomics* 4 (2012) 568–575.
- [17] A.K. Gorle, J. Zhang, Q. Liu, S.J. Berners-Price, N.P. Farrell, *Chem. Eur. J.* 26 (2018) 4643–4652.
- [18] S.D. Tsotsoros, P.B. Lutz, A.G. Daniel, E.J. Peterson, R.E.F. de Paiva, E. Rivera, Y. Qu, C.A. Bayse, N.P. Farrell, *Chem. Sci.* 8 (2017) 1269–1281.
- [19] S.D. Tsotsoros, A.B. Bate, M.G. Dows, S.R. Spell, C.A. Bayse, N.P. Farrell, *J. Inorg. Biochem.* 132 (2014) 2–5.
- [20] S.D. Tsotsoros, Y. Qu, N.P. Farrell, *J. Inorg. Biochem.* 143 (2015) 117–122.
- [21] J.A. Plumb, B. Venugopal, R. Oun, N. Gomez-Roman, Y. Kawazoe, N.S.

- Venkataramanan, N.J. Wheate, *Metallomics* 4 (2012) 561–567.
- [22] M.J. Pisani, Y. Zhao, L. Wallace, C.E. Woodward, F.R. Keene, A.I. Day, J.G. Collins, *Dalton Trans.* 39 (2010) 2078–2086.
- [23] N.L. McGinely, J.A. Plumb, N.J. Wheate, *J. Inorg. Biochem.* 128 (2013) 124–130.
- [24] Z.-F. Chen, Q.-P. Qin, J.-L. Qin, J. Zhou, Y.-L. Li, N. Li, Y.-C. Liu, H. Liang, J. *Med. Chem.* 58 (2015) 4771–4789.
- [25] T. Tauchi, K. Shin-ya, G. Sashida, M. Sumi, S. Okabe, J.H. Ohyashiki, K. Ohyashiki, *Oncogene* 25 (2006) 5719–5725.
- [26] Q. Li, J. Zhang, L. Yang, Q. Yu, Q. Chen, X. Qin, F. Le, Q. Zhang, J. Liu, *J. Inorg. Biochem.* 130 (2014) 122–129.
- [27] C.-X. Xu, Y. Shen, Q. Hu, Y.-X. Zheng, Q. Cao, P.Z. Qin, Y. Zhao, L.-N. Ji, Z.-W. Mao, *Chem. Asian J.* 9 (2014) 2519–2526.
- [28] D.-L. Ma, C.-M. Che, S.-C. Yan, *J. Am. Chem. Soc.* 131 (2009) 1835–1846.
- [29] J.E. Reed, S. Neidle, R. Vilar, *Chem. Commun.* (2007) 4366–4368.
- [30] K. Paul, S. Bindal, V. Luxami, *Bioorg. Med. Chem. Lett.* 23 (2013) 3667–3672.
- [31] S. Cosconati, A. Rizzo, R. Trotta, B. Pagano, S. Iachettini, S. De Tito, I. Lauri, I. Fotticchia, M. Giustiniano, L. Marinelli, C. Giancola, E. Novellino, A. Biroccio, A. Randazzo, *J. Med. Chem.* 55 (2012) 9785–9792.
- [32] W. Wu, W. Wu, S. Ji, H. Guo, J. Zhao, *Dalton Trans.* 40 (2011) 5953–5963.
- [33] M. Ali, L. Dondaine, A. Adolle, C. Sampaio, F. Chotard, P. Richard, F. Denat, A. Bettaieb, P. Le Gendre, V. Laurens, C. Goze, C. Paul, E. Bodio, *J. Med. Chem.* 58 (2015) 4521–4528.
- [34] H.S. Jung, P.S. Kwon, J.W. Lee, J.I. Kim, C.S. Hong, J.W. Kim, S. Yan, J.Y. Lee, J.H. Lee, T. Joo, J.S. Kim, *J. Am. Chem. Soc.* 131 (2009) 2008–2012.

- [35] Q.-P. Qin, S.-L. Wang, M.-X. Tan, Z.-F. Wang, X.-L. Huang, Q.M. Wei, B.-B. Shi, B.-Q. Zou, H. Liang, *Metallomics* 10 (2018) 1160–1169.
- [36] R.M. Christie, C.H. Lui, *Dyes and Pigments* 47 (2000) 79–89.
- [37] S. Madonna, A. Marcowycz, D. LamoralpTheys, G. Van Goietsenoven, J. Dessolin, C. Pirker, S. Spiegl-Kreinecker, C.-A. Biraboneye, W. Berger, R. Kiss, J.-L. Kraus, *J. Heterocycl. Chem.* 47 (2010) 719–723.
- [38] R. Cao, J.-L. Jia, X.-C. Ma, M. Zhou, H. Fei, *J. Med. Chem.* 56 (2013) 3636–3644.
- [39] A. Ali, M. Kamra, S. Roy, K. Muniyappa, S. Bhattacharya, *Bioconjugate Chem.* 28 (2017) 341–352.
- [40] K. Yadav, P.N.R. Meka, S. Sadhu, S.D. Guggilapu, J. Kovvuri, A. Kamal, R. Srinivas, P. Devayani, B.N. Babu, N. Nagesh, *Biochemistry.* 56 (2017) 4392–4404.
- [41] H.U. Holtkamp, S. Movassaghi, S.J. Morrow, M. Kubanik, C.G. Hartinger, *Metallomics* 10 (2018) 455-462.
- [42] C.A. Puckett, J.K. Barton, *J. Am. Chem. Soc.* 129 (2007) 46–47.
- [43] Q.-P. Qin, J.-L. Qin, T. Meng, W.-H. Lin, C.-H. Zhang, Z.-Z. Wei, J.-N. Chen, Y.-C. Liu, H. Liang, Z.-F. Chen, *Eur. J. Med. Chem.* 124 (2016) 380–392.
- [44] S.H. van Rijt, A. Mukherjee, A.M. Pizarro, P.J. Sadler, *J. Med. Chem.* 53 (2010) 840–849.
- [45] S.K. Bhal, K. Kassam, I.G. Peirson, G.M. Pearl, *Mol. Pharmaceutics* 4 (2007) 556–560.
- [46] J.A. Platts, D.E. Hibbs, T.W. Hambley, M.D. Hall, *J. Med. Chem.* 44 (2001) 472–474.
- [47] Y.-R. Zheng, K. Suntharalingam, T.C. Johnstone, H. Yoo, W. Lin, J.G. Brooks,

- S.J. Lippard, *J. Am. Chem. Soc.* 136 (2014) 8790–8798.
- [48] S.P. Oldfield, M.D. Hall, J.A. Platts, *J. Med. Chem.* 50 (2007) 5227–5237.
- [49] Z.-F. Chen, Q.-P. Qin, J.-L. Qin, Y.-C. Liu, K.-B. Huang, Y.-L. Li, T. Meng, G.-H. Zhang, Y. Peng, X.-J. Luo, H. Liang, *J. Med. Chem.* 58 (2015) 2159–2179.
- [50] D.-Y. Zeng, G.-T. Kuang, S.-K. Wang, W. Peng, S.-L. Lin, Q. Zhang, X.-Xuan Su, M.-H. Hu, H. Wang, J.-H. Tan, Z.-S. Huang, L.-Q. Gu, T.-M. Ou, *J. Med. Chem.* 60 (2017) 5407–5423.
- [51] M. Chalfie, Y. Tu, G. Euskirchen, W.W. Ward, D.C. Prasher, *Science* 263 (1994) 802–805.
- [52] T.-C. He, A.B. Sparks, C. Rago, H. Hermeking, L. Zawel, L.T. da Costa, P.J. Morin, B. Vogelstein, K.W. Kinzler, *Science* 281 (1998) 1509–1512.
- [53] L. Zhou, L. Jiang, M. Xu, Q. Liu, N. Gao, P. Li, E.-H. Liu, *Sci. Rep.* 6 (2016) 20585; doi: 10.1038/srep20585.
- [54] J. Jacobson, M.R. Duchon, *J. Cell Sci.* 115 (2002) 1175–1188.
- [55] G. Petrosillo, F.M. Ruggiero, M. Pistolese, G. Paradies, *J. Biol. Chem.* 279 (2004) 53103–53108.
- [56] S. Shrivastava, M.K. Jeengar, V.S. Reddy, G.B. prakash Reddy, V.G.M. Naidu, *Exp. Mol. Pathol.* 98 (2015) 313–327.
- [57] G.-B. Jiang, X. Zheng, J.-H. Yao, B.-J. Han, W. Li, J. Wang, H.-L. Huang, Y.-J. Liu, *J. Inorg. Biochem.* 141 (2014) 170–179.
- [58] G. M. Sheldrick, SHELXTL-97, Program for refinement of crystal structures, University of Göttingen, Germany, 1997.
- [59] H.-H. Zou, L. Wang, Z.-X. Long, Q.-P. Qin, Z.-K. Song, T. Xie, S.-H. Zhang, Y.-C. Liu, B. Lin, Z.-F. Chen, *Eur. J. Med. Chem.* 108 (2016) 1–12.
- [60] L. Xu, X. Chen, J. Wu, J. Wang, L. Ji, H. Chao, *Chem. Eur. J.* 21 (2015) 4008–

4020.

- [61] J.-L. Qin, Q.-P. Qin, Z.-Z. Wei, C.-C. Yu, T. Meng, C.-X. Wu, Y.-L. Liang, H. Liang, Z.-F. Chen, *Eur. J. Med. Chem.* 124 (2016) 417–427.
- [62] J.S. Butler, P.J. Sadler, *Curr. Opin. Chem. Biol.* 17 (2013) 175–188.
- [63] D.K. Heidary, B.S. Howerton, E.C. Glazer, *J. Med. Chem.* 57 (2014) 8936–8946.
- [64] Q.-P. Qin, T. Meng, M.-X. Tan, Y.-C. Liu, X.-J. Luo, B.-Q. Zou, H. Liang, *Eur. J. Med. Chem.* 143 (2018) 1597–1603.

### Figure Captions:

**Fig. 1.** The molecular structures of the **Pt1**.

**Fig. 2.** TRAP assay performed in the presence of **Pt1** (1.0  $\mu\text{M}$ ), **Pt2** (3.0  $\mu\text{M}$ ), **Pt3** (10.0  $\mu\text{M}$ ), **Pt4** (3.0  $\mu\text{M}$ ) and **Pt5** (10.0  $\mu\text{M}$ ) in SK-OV-3/DDP cancer cells, respectively.

**Fig. 3.** ICP-MS data for SK-OV-3/DDP cancer cells incubated with **Pt1** (1.0  $\mu\text{M}$ ), **Pt2** (3.0  $\mu\text{M}$ ), **Pt3** (10.0  $\mu\text{M}$ ) and cisplatin (15.0  $\mu\text{M}$ ), respectively.

**Fig. 4.** Induction of telomerase activity by **Pt1** (1.0  $\mu\text{M}$ ), **Pt2** (3.0  $\mu\text{M}$ ), **Pt3** (10.0  $\mu\text{M}$ ) via c-myc promoter elements activation. (A) The expression percentage of the hTERT and c-myc genes after 24 h of incubation of SK-OV-3/DDP tumor cells with the Pt(II) complexes **Pt1** (1.0  $\mu\text{M}$ ), **Pt2** (3.0  $\mu\text{M}$ ) and **Pt3** (10.0  $\mu\text{M}$ ) as determined by means of the RT-qPCR assay. (B) Western blot analysis of hTERT and c-myc expression in the SK-OV-3/DDP tumor cells with the Pt(II) complexes **Pt1** (1.0  $\mu\text{M}$ ), **Pt2** (3.0  $\mu\text{M}$ ) and **Pt3** (10.0  $\mu\text{M}$ ). (C) The whole cell extracts were prepared and analyzed by Western blot analysis using antibodies against hTERT and c-myc proteins. The same blots

were stripped and re probed with a  $\beta$ -actin antibody to show equal protein loading. Western blotting bands from three independent measurements were quantified with Image J. in (C). Transfection of 2.0 mg EGFP (enhanced green fluorescent protein) plasmid (D) and 2.0 mg c-myc plasmid vectors (E) in the SK-OV-3/DDP tumor cells treated with the Pt(II) complexes **Pt1** (1.0  $\mu$ M), **Pt2** (3.0  $\mu$ M) and **Pt3** (10.0  $\mu$ M) for 24.0 h, respectively, and these results was assessed by fluorescence microscopy or Multimodel Plate Reader with luciferase reporter gene assay kit.

**Fig. 5.** (A) Intracellular ROS levels in SK-OV-3/DDP tumor cells exposed to the Pt(II) complexes **Pt1** (1.0  $\mu$ M), **Pt2** (3.0  $\mu$ M) and **Pt3** (10.0  $\mu$ M) for 24 h and the DCF fluorescent intensity was determined by flow cytometric analysis, respectively. (B) Effects of the Pt(II) complexes **Pt1** (1.0  $\mu$ M), **Pt2** (3.0  $\mu$ M) and **Pt3** (10.0  $\mu$ M) on  $\text{Ca}^{2+}$  activation level in SK-OV-3/DDP tumor cells.

**Fig. 6.** The Pt(II) complexes **Pt1** (1.0  $\mu$ M), **Pt2** (3.0  $\mu$ M) and **Pt3** (10.0  $\mu$ M) induced depletion of mitochondrial membrane potential ( $\Delta\psi$ m) in SK-OV-3/DDP tumor cells. These cells were treated with the Pt(II) complexes **Pt1** (1.0  $\mu$ M), **Pt2** (3.0  $\mu$ M) and **Pt3** (10.0  $\mu$ M) for 24 h and then analyzed by JC-1 flow cytometry.

**Fig. 7.** (A) The SK-OV-3/DDP tumor cells were treated with the Pt(II) complexes **Pt1** (1.0  $\mu$ M), **Pt2** (3.0  $\mu$ M) and **Pt3** (10.0  $\mu$ M) for 24 h and the expression levels of the apoptosis-related proteins were examined by Western blotting. (B) The whole cell extracts were prepared and analyzed by Western blot analysis using antibodies against the apoptosis related proteins. The same blots were stripped and re probed with a  $\beta$ -actin antibody to show equal protein loading. Western blotting bands from three independent measurements were quantified with Image J. in (B).

**Fig. 8.** Apoptosis of SK-OV-3/DDP tumor cells induced by the Pt(II) complexes **Pt1** (1.0  $\mu$ M), **Pt2** (3.0  $\mu$ M) and **Pt3** (10.0  $\mu$ M) for 24 h, respectively.

**Scheme 1.** Synthetic routes for substituted 3-(2'-benzimidazolyl)coumarins platinum(II) complexes **Pt1–Pt8**. (a) piperidine, EtOH, 55°C for 24 h; (b) 2.0% HCl, reflux, 6.0 h; (c) *cis*-Pt(DMSO)<sub>2</sub>Cl<sub>2</sub>, CH<sub>3</sub>OH/DMSO (v/v=2.0 /0.5mL), 90°C for 24 h.

**Table 1.** IC<sub>50</sub><sup>a</sup> (μM) values of cisplatin, the ligands MeOBC, OHBC, BC, FBC, BrBC, FFBC, ClCIBC, BrBrBC, the Pt(II) complexes **Pt1–Pt8** against the five human cells for 48 h.

Compounds	HeLa	Hep-G2	SK-OV-3/DDP	SK-OV-3	HL-7702
MeOBC	30.19 ± 0.63	>100	90.06 ± 0.41	>100	>100
<b>Pt1</b>	5.26 ± 0.87	25.69 ± 0.46	1.01 ± 0.27	19.89 ± 1.46	>100
OHBC	38.06 ± 1.03	>100	>100	>100	>100
<b>Pt2</b>	7.21 ± 1.45	35.26 ± 1.43	3.26 ± 1.06	28.06 ± 1.27	>100
BC	>100	>100	>100	>100	>100
<b>Pt3</b>	58.79 ± 0.56	>100	10.32 ± 0.66	86.36 ± 1.65	>100
FBC	40.02 ± 1.85	>100	>100	>100	>100
<b>Pt4</b>	10.23 ± 0.45	45.26 ± 1.06	5.15 ± 0.59	35.29 ± 0.77	>100
BrBC	56.23 ± 1.21	>100	>100	>100	>100
<b>Pt5</b>	16.02 ± 0.47	50.11 ± 1.44	8.02 ± 1.19	40.11 ± 1.17	>100
FFBC	68.16 ± 0.91	>100	>100	>100	>100
<b>Pt6</b>	25.12 ± 1.17	86.03 ± 0.55	8.69 ± 0.83	57.56 ± 1.49	>100
ClCIBC	78.02 ± 0.55	>100	>100	>100	>100
<b>Pt7</b>	31.25 ± 1.52	>100	9.16 ± 1.59	65.22 ± 0.61	>100
BrBrBC	86.34 ± 1.70	>100	>100	>100	>100
<b>Pt8</b>	41.51 ± 1.02	>100	9.86 ± 0.54	72.06 ± 1.45	>100
Cisplatin <sup>b</sup>	15.09 ± 1.19	12.06 ± 0.91	70.26 ± 1.93	17.12 ± 0.59	16.24 ± 0.63

<sup>a</sup> IC<sub>50</sub> values are presented as the mean ± SD (standard error of the mean) from five independent experiments. <sup>b</sup> Cisplatin was dissolved at a concentration of 1.0 mM in 0.154 M NaCl [37, 38].

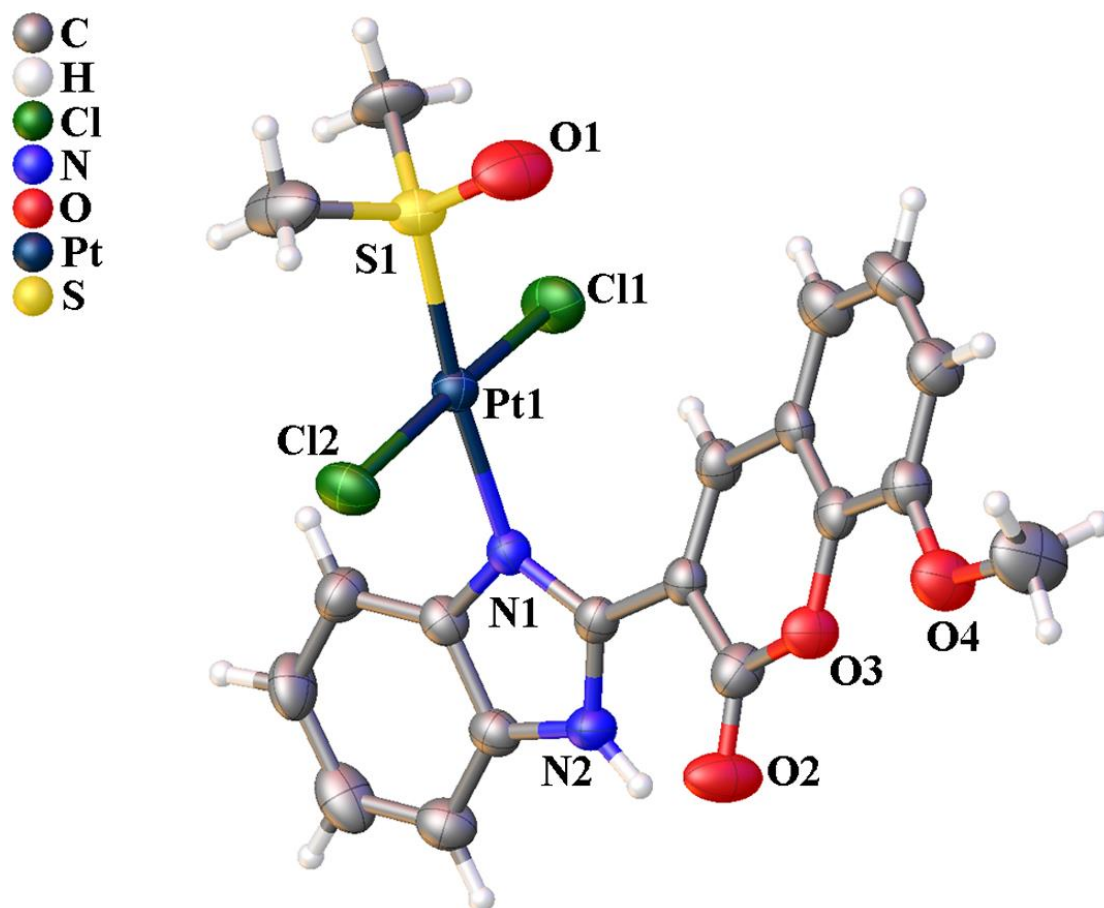


Fig. 1



Fig. 2

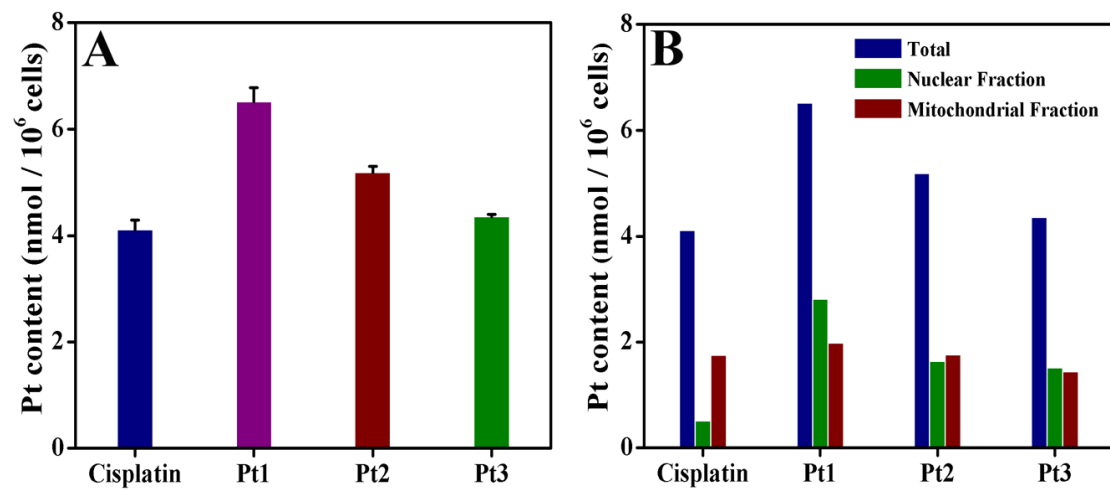


Fig. 3

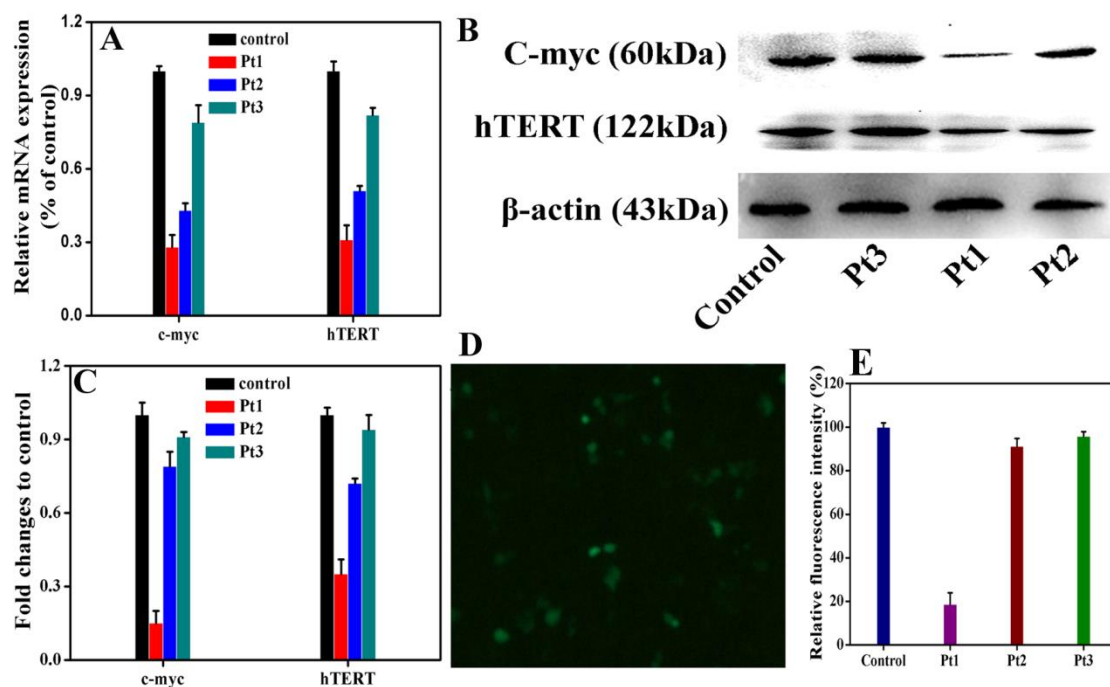


Fig. 4

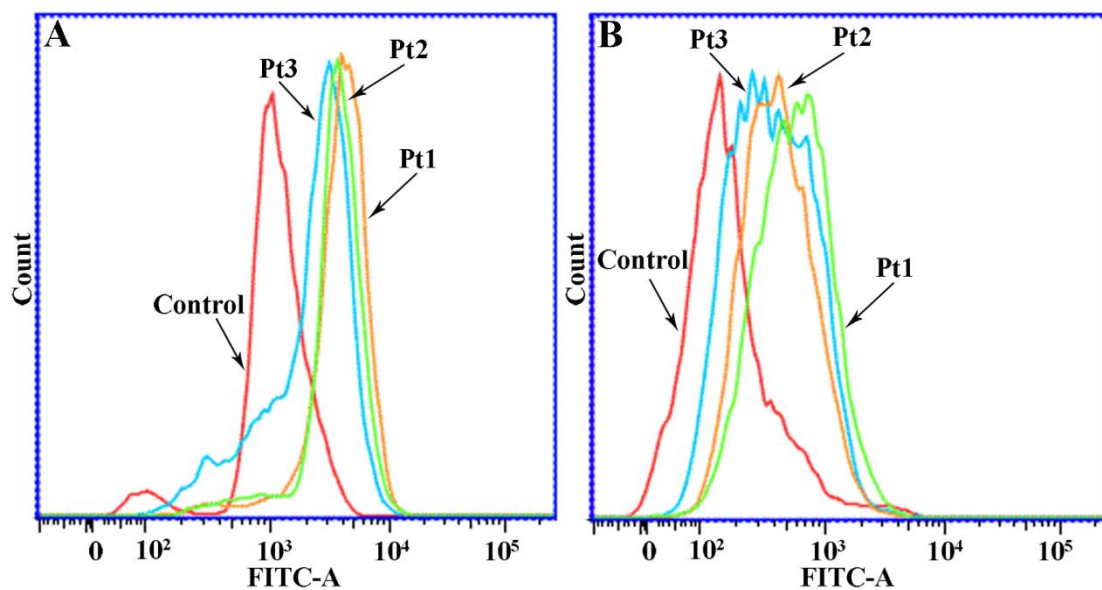


Fig. 5

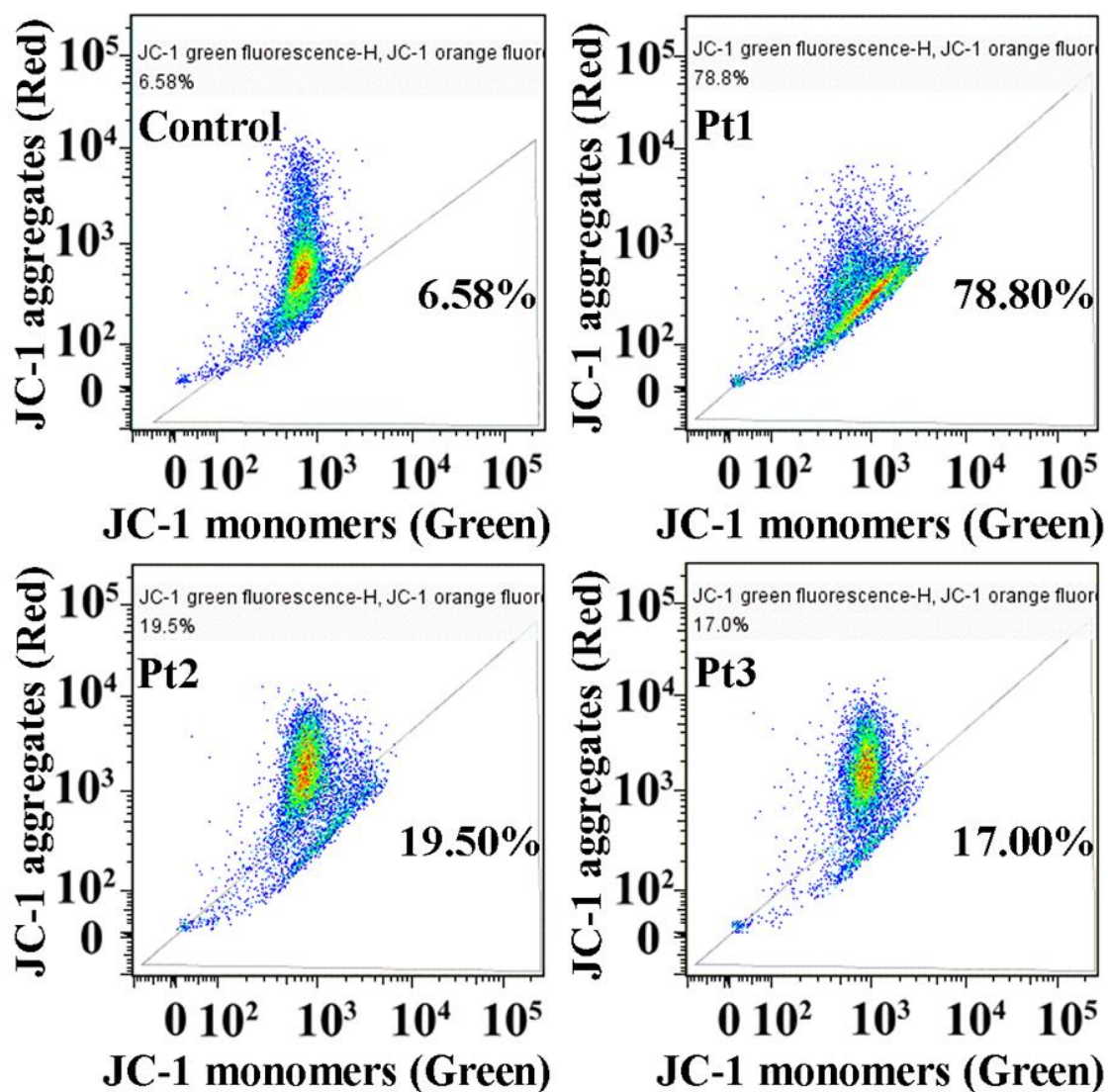


Fig. 6

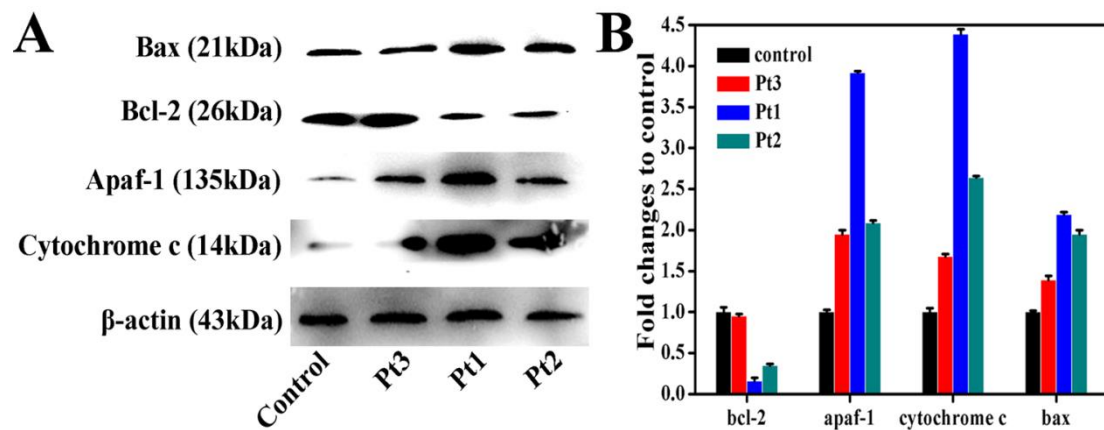


Fig. 7

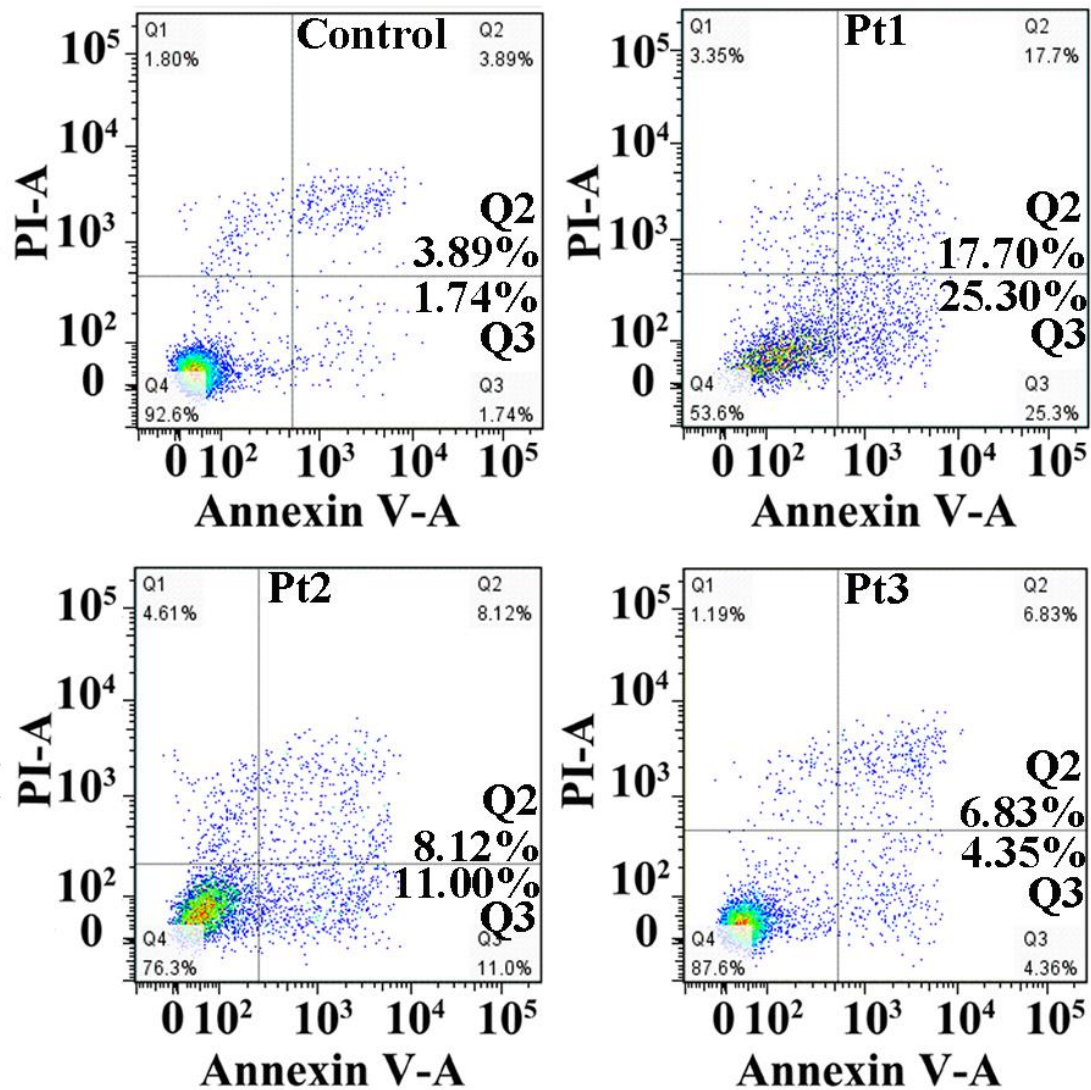
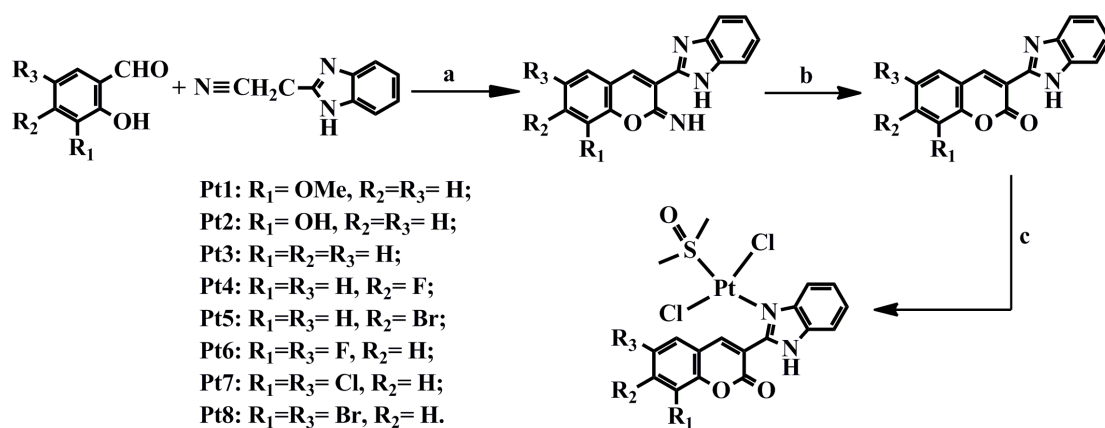


Fig. 8

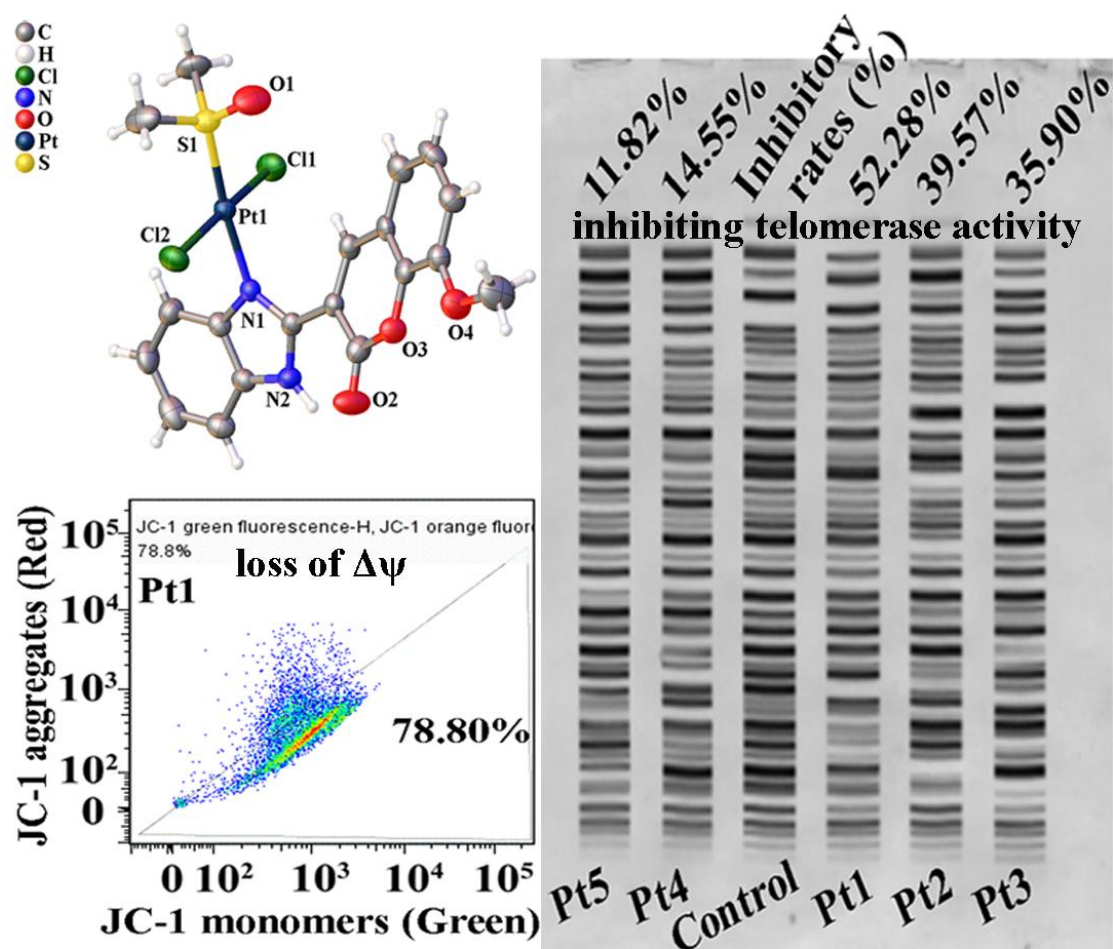


Scheme 1

## Graphical abstract

# Synthesis and biological evaluation of substituted 3-(2'-benzimidazolyl)coumarin platinum(II) complexes as new telomerase inhibitors

Ting Meng <sup>a</sup>, Qi-Pin Qin <sup>a,b,\*</sup>, Zhen-Rui Wang <sup>a</sup>, Li-Ting Peng <sup>a</sup>, Hua-Hong Zou <sup>a,\*</sup>,  
Zhen-Yuan Gan <sup>a</sup>, Ming-Xiong Tan <sup>b,\*</sup>, Kai Wang <sup>c</sup>, Fu-Pei Liang <sup>a,c,\*</sup>



Eight new platinum(II) complexes **Pt1–Pt8** with substituted 3-(2'-benzimidazolyl) coumarins were synthesized and characterized. **Pt1** is a telomerase inhibitor targeting c-myc promoter elements and causes mitochondrial dysfunction in the following order: **Pt1>Pt2>Pt3**.

**Highlights:**

- These complexes, **Pt1–Pt8**, were structurally and spectroscopically characterized.
- SK-OV-3/DDP cells were found to be the most sensitive towards **Pt1–Pt8**.
- **Pt1–Pt3** also caused mitochondrial dysfunction.
- **Pt1** was a telomerase inhibitor targeting c-myc promoter elements.